Design and reliability analysis of four-legged jacket type offshore platform in Java Sea

Siti N. Kaban[1,5,*], Sandy H. S. Herho[2,3], Dasapta E. Irawan[4], and Ricky L. Tawekal[5]

[1]School of Architecture, Planning and Preservation, University of Maryland, College Park
[2]Department of Geology, University of Maryland, College Park
[3]Department of Earth and Planetary Sciences, University of California, Riverside
[4]Applied Geology Research Group, Bandung Institute of Technology
[5]Offshore Engineering Research Group, Bandung Institute of Technology
[*]Corresponding author: kabansn@umd.edu

Abstract

In the design process of offshore platforms in Indonesia, random variables of load and material strength must be taken into account. To cover this uncertainty, the industry standard in Indonesia is to use the American Petroleum Institute Recommended Practice 2A-LRFD (API RP2A-LRFD) load factor. To further assess the reliability of the structure, a structural design analysis was carried out according to the provisions of API RP2A-LRFD, and the Monte Carlo method was used to determine the reliability index of the structure. This would help to determine whether the structural design is conservative or not according to the LRFD load factor. Additionally, four important members of the structure were selected to assess the reliability of the structure against the random variables of load and material strength. With the reliability index, it will be possible to have an overview of the structural design and ensure that the structure is safe and secure against environmental conditions in Indonesia.

1 Introduction

Offshore platforms are used in oil and gas exploration and production and can be fixed to the seabed or float (Qiu, 2007). This project uses a four-legged jacket type structure fixed to the Java Sea seabed, with a water depth of 100 ft from the mean sea level (m.s.l.). The structure must meet the American Petroleum Institute Recommended Practice 2A-LRFD (API RP2A-LRFD) criteria (Turner et al., 1994), and therefore three analyses must be conducted: an in-place analysis, a seismic analysis, and a fatigue analysis (Shittu et al., 2021). In the In-place analysis, Cross-sectional optimization is carried out on the structure, and a Reliability analysis is conducted to assess the structure's probability of failure (P_f) with the given load and structural resistance (Qiu, 2007). This approach provides an initial indication of the API RP2A-LRFD design load factor in the Java Sea, and the structural members' reliability index (β) would be obtained.

In this study, structural modeling was conducted using the Bentley Structural Analysis Computer System (SACS) Offshore Structure software to account for the structure, equipment, and environmental load. This software has proven to be used successfully to analyze and design offshore structures in various places in the world (e.g. Karimi et al., 2017; Ozkul et al., 2021; Lakhani and Panchal, 2022; Raheem et al., 2022; Tran et al., 2022). Furthermore, the design process was completed based on in-place analysis criteria and seismic and fatigue analysis (Turner et al., 1994). Member stress checks, joint punching shears, and pile capacity checks were carried out. If there was a structural failure, a cross-section redesign was implemented to meet the API RP2A-LRFD design criteria (Turner et al., 1994). In addition, reliability analysis was conducted on four important members, each representing the four main parts of the structure. To this end, data on significant wave height from generated sea-fine was used as the random variable load, and the yield strength of degenerated steel based on ISO 19902 parameters were used as the random variable strength. The Monte Carlo method was then employed to calculate the reliability index value (β), which is the condition of the member stress performance in in-place analysis (Turner et al., 1994; ISO 19902, 2007; Barthelmie et al., 2016). Figure 1 summarizes the overall stages of this project. This study analyzed an offshore platform structure with a four-legged jacket type. It was installed in the waters of the Java Sea, located at coordinates $108.671389°$E, $6.3375°$S. This location is in the northern part of Cirebon and the east of Indramayu (Figure 2). The water depth at this location is 100 ft from the datum m.s.l to the seabed.

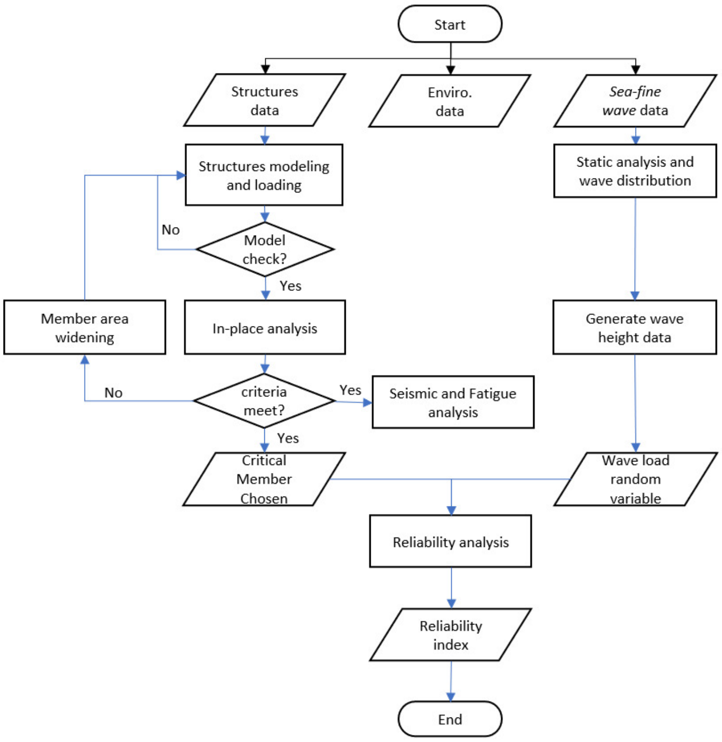

Figure 1: Project flowchart.

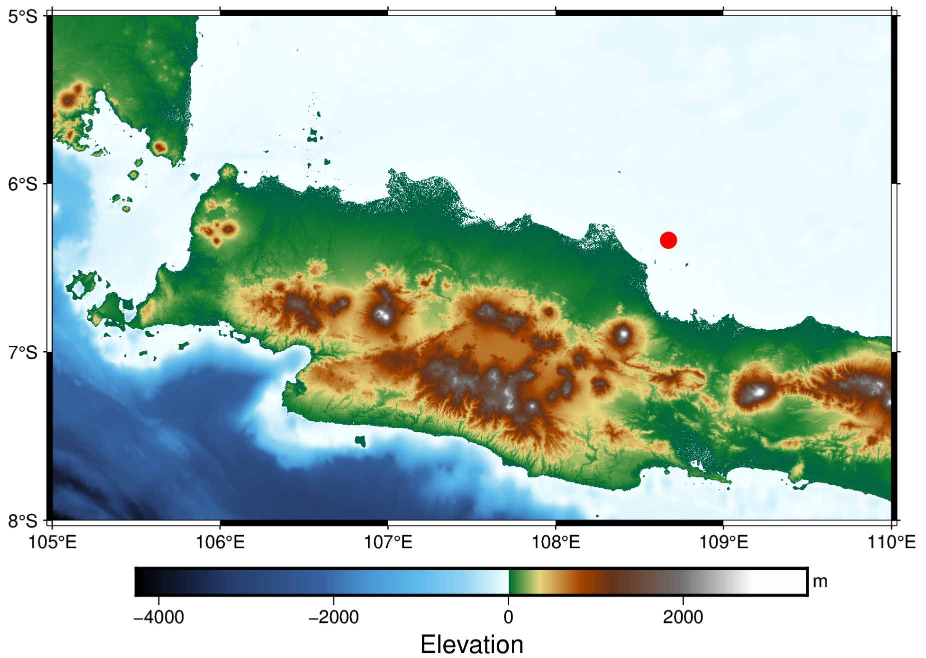

Figure 2: Platform location off the coast of the Java Sea (red dot). This map was rendered using PyGMT (Wessel et al., 2019; Uieda et al., 2023).

The bridge structure has three decks:

- main deck at $+45$ ft,
- mezzanine deck at $+31$ ft,

- cellar deck at $+25$ ft.

The working point is at $+15$ ft elevation, and the jacket walkway is at $+10$ ft elevation. Figure 3 illustrates the structure of the bridge. Environmental data such as wind, current, and wave were used to perform the analysis. Table 1 shows the wind data used in the process. Since the flow data above is a single dataset on the water surface (0 m.s.l.), the current data must be distributed to generate distributed flow data (Table 2).

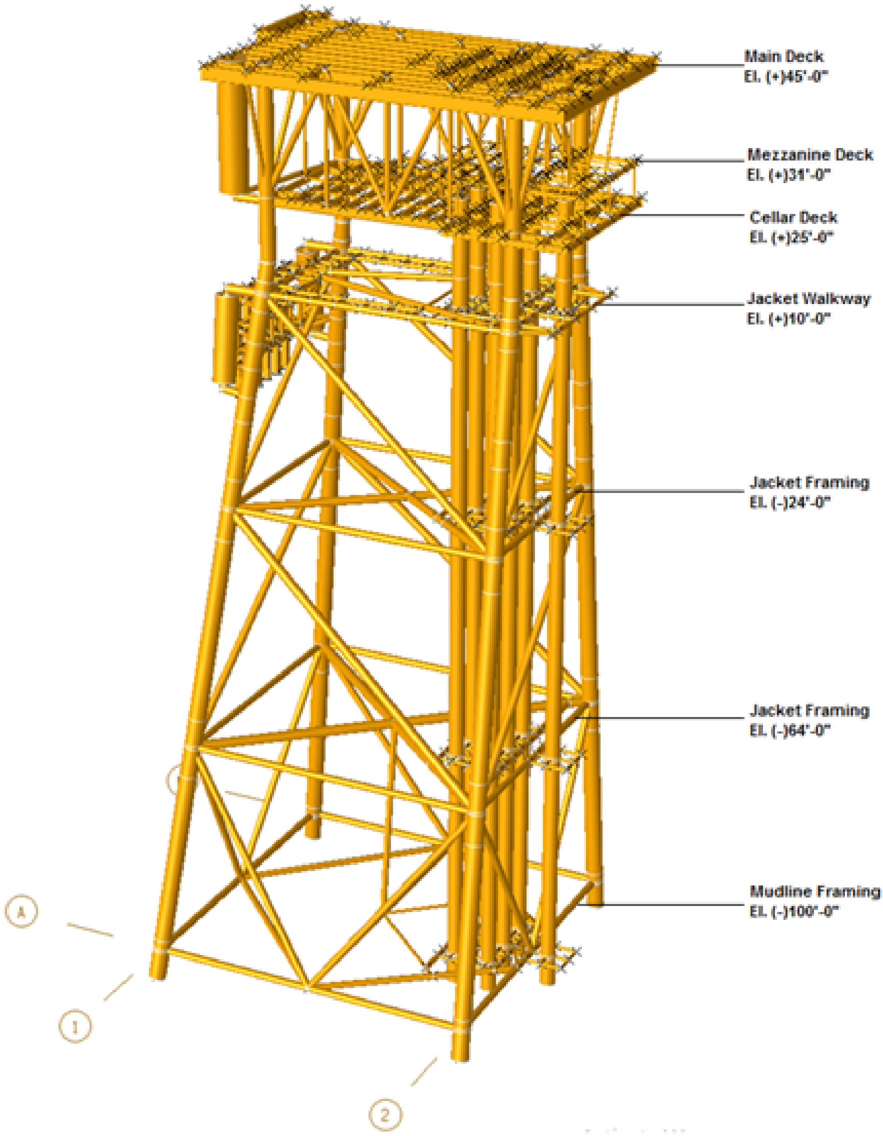

Figure 3: Four-legged jacket type structural model in Bentley SACS.

condition	wind speed (ft/sec.)	wave H_{max} (ft)	wave T_{max} (sec.)	wave speed (ft/sec.)
1-year operating	42.19	14.83	8	2.07
100-year extreme	56.14	20.87	9.1	2.56

Table 1: Environmental data.

Z (ft)	operating U_Z (ft/sec.)	storm U_Z (ft/sec.)
0	0	0
10	1.49	1.842
20	1.645	2.034
30	1.743	2.155
40	1.816	2.246
50	1.875	2.319
60	1.924	2.38
70	1.967	2.433
80	2.005	2.48
90	2.039	2.522
100	2.07	2.56

Table 2: Current distribution.

2 Structural analysis

2.1 In-place analysis

The in-place analysis in the design process included member stress checks, joint punching shear inspections, and pile axial capacity checks based on the API RP2A-LRFD criteria. Two loading conditions were considered: Operating and Storm. Unity Check (UC) values were calculated, and a safe design criterion of UC less than 1 was applied. For the pile capacity inspection, the load on the pile must be below the factored pile capacity, with a factor of 0.7 for operating conditions and 0.8 for storm conditions (Turner et al., 1994; Mangiavacchi et al., 2005; Digre and Zwerneman, 2012). The results of the in-place analysis for the respective operating and storm conditions are presented in Tables 3 to 6. All load values were below the factored capacity value, indicating that the structure meets the design criteria for both operating and storm conditions. Therefore, the overall structural design examination based on the in-place analysis was successful.

location	member	group	property	$UC_{min.}$	$UC_{max.}$
main deck	M397-M030	MA2	W24×68	0.851	0.85
cellar deck	C024-C029	CL4	C 8×11.5	0.574	0.576
mezzanine deck	Z037-Z016	ME2	L4×4$^1/_4$	0.963	0.964
deck leg	603L-C003	DL1	OD30”×1”WT	0.394	0.396
deck brace	C002-M015	TR1	OD10.75”×0.365”WT	0.685	0.678
jacket leg	0026-0038	LG2	OD34”×0.5”WT	0.375	0.363
jacket brace	304L-403L	DG2	OD16”×0.375”WT	0.582	0.605
pile	301P-401P	PL1	OD30”×1”WT	0.377	0.357

Table 3: UC member operating.

location	member	group	property	$UC_{min.}$	$UC_{max.}$
main deck	M054-M057	MA3	W16×21	0.734	0.727
cellar deck	C132-C133	CL1	C16×67	0.927	0.927
mezzanine deck	0092-Z027	ME2	L4×4$^1/_4$	0.664	0.663
deck leg	602L-C002	DL1	OD30”×1”WT	0.418	0.412
deck brace	C002-M015	TR1	OD10.75”×0.365”WT	0.623	0.614
jacket leg	0025-0037	LG2	OD34”×0.5”WT	0.483	0.483
jacket brace	304L-403L	DG2	OD16”×0.375”WT	0.818	0.842
pile	301P-401P	PL1	OD30”×1”WT	0.555	0.537

Table 4: UC member storm.

operating condition			storm condition		
joint	$UC_{min.}$	$UC_{max.}$	joint	$UC_{min.}$	$UC_{max.}$
403L	0.630	0.704	304L	0.481	0.481
402L	0.569	0.554	303L	0.395	0.389
304L	0.492	0.492	302L	0.359	0.364

Table 5: UC joint can.

pile joint	capacity (QD)	0.8 (QD)	operating		storm	
			water level max.	water level min.	water level max.	water level min.
(Kips)	(Kips)	(Kips)	(Kips)	(Kips)	(Kips)	(Kips)
001P	1500.4	1200.32	690.5	711.5	787.3	806.4
002P	1506.2	1204.96	690.5	521.8	400	402.5
003P	1500.4	1200.32	599.8	611.6	723.2.3	733.4
004P	1506.2	1204.96	790.4	805.4	758.4	772.1

Table 6: pile capacity

2.2 Seismic analysis

Dynamic analysis was used to assess the seismic conditions of the structure. The structure's natural period was determined to be 2.03 sec., with 90% of the mass participation in the 12th mode. Table 7 displays the value of each Pseudo Spectrum (PSV) of the two earthquake loads; Strength Level Earthquake (SLE, PGA $= 0.159g$) and Ductility Level Earthquake (DLE, PGA $= 0.239g$).

period	PSV_{SLE} (in/s/g)	PSV_{DLE} (in/s/g)
0.03	1.845	1.845
0.05	3.075	3.075
0.125	15.238	15.238
0.5	54.714	60.952
5	54.714	60.952
10	23.357	30.476

Table 7: Response spectra.

Tables 8 to 10 display the results of the member stress UC, joint punching shear, and pile capacity checks for the SLE and DLE earthquake conditions. The pile capacity met both operating and storm conditions for each maximum and minimum water level, as the working load was below the factored capacity value. Based on the seismic analysis, it can be concluded that the structure has met the design criteria for SLE and DLE earthquake conditions. This evidence is supported by the findings of Khatibi et al. (2014), which determined that structures must satisfy the design criteria for seismic conditions to remain safe and secure.

location	member	group	property	$UC_{SLE.}$	$UC_{DLE.}$
main deck	M021-M001	MA2	W24×68	0.503	0.555
cellar deck	C057-C085	CL4	C8×11.5	0.460	0.556
mezzanine deck	0092-Z027	ME2	L4×4$^1/_4$	0.519	0.532
deck leg	602L-C002	DL1	OD30"×1"WT	0.310	0.406
deck brace	C003-M008	TR1	OD10.75"×0.365"WT	0.416	0.558
jacket leg	0026-0038	LG2	OD34"×0.5"WT	0.253	0.342
jacket brace	304L-403L	DG2	OD16"×0.375"WT	0.463	0.685
pile	301P-401P	PL1	OD30"×1"WT	0.332	0.444

Table 8: UC member values.

joint	UC_{SLE}	UC_{DLE}
304L	0.688	0.688
303L	0.421	0.421
401L	0.386	0.386
204L	0.334	0.334

Table 9: UC joint can values.

pile joint	capacity (QD) (Kips)	0.7 (QD) (Kips)	DLE load (Kips)	SLE load (Kips)
001P	1432.35	1002.645	701.06	569.19
002P	1432.35	1002.645	370.47	328.88
003P	1432.35	1002.645	587.23	450.26
004P	1432.35	1002.645	778.38	637.39

Table 10: Pile capacity.

2.3 Fatigue analysis

Fatigue analysis is a critical stage of the design analysis process. It helps determine the service life of a joint structure by analyzing the effect of cyclic environmental loads on it. The analysis involves providing the system with different wave heights, wave periods, and directions (eight directions) (Bai, 2003a; Chen et al., 2016; Plodpradit et al., 2019; Sánchez et al., 2019). The fatigue analysis output is the joint structure's service life, which is determined by the damage value of the design upon its exposure to cyclic loads.

The fatigue analysis results for the joint structure are presented in Tables 11 and 12. The damage value for the joint structure was above 1, indicating that further assessment of the jacket bracing members is necessary to survive the desired service life of 52 years (Lee et al., 2023). Table 12 displays the fatigue life values for the other joints below 1.

joint	member	group	damage	fatigue life (year)
0006	102L-0006	BR3	1.67	31

Table 11: Fatigue life (damage > 1).

joint	member	group	damage	fatigue life (year)
003P	003P-103P	PL1	0.85	61.11
304L	202L-304L	DG3	0.64	81.27
304L	0032-304L	LG1	0.54	96.57
604L	504L-604L	PL1	0.53	98.06
0163	0165-0163	HR3	0.28	184.40
303L	303L-304L	HR1	0.21	248.80

Table 12: Fatigue life (damage < 1).

3 Reliability analysis

Reliability analysis is a crucial step in this study. Based on the criteria presented in Table 13, four main members were selected for the analysis. Reliability is defined as the probability of success (P_s) that meets the performance criteria expressed in the performance function as follows,

$$Z = g(X_1, X_2, \cdots, X_n) \tag{1}$$

, where X_i defines a random variable related to load and capacity parameters. Two random variables, structural strength and load, were selected to determine the performance failure parameters. Therefore, the performance function used was,

$$g(R, Q) = R - Q \tag{2}$$

, where R defines the parameter of the strength of the structure, and Q is the parameter of the structure's load. The structure's failure probability is when $g(R, Q) < 0$.

location	factored		unfactored	
main beam	mean	0.5917	mean	0.3753
	standard error	0.0044	standard error	0.0029
	COV	0.0525	COV	0.0540
deck leg	mean	0.3197	mean	0.2006
	standard error	0.0024	standard error	0.0016
	COV	0.0524	COV	0.0547
jacket leg	mean	0.2615	mean	0.1784
	standard error	0.0029	standard error	0.0021
	COV	0.0764	COV	0.0826
pile	mean	0.2552	mean	0.1662
	standard error	0.0029	standard error	0.0021
	COV	0.0790	COV	0.0875

Table 13: UC statistical parameters

The structural strength parameter selected was the yield stress of the structural material (F_y), and the load parameter was a wave load with significant wave height and period. Monte Carlo simulation (Alpers, 1983; Guo et al., 2012; Clarindo et al., 2021; Görmüş et al., 2022) was used as the reliability analysis method, with 50 simulations carried out. To generate the wave data, 59 years of significant wave data from the Java Sea was used to determine the wave data distribution. Kolmogorov-Smirnov (K-S) method (Massey Jr., 1951) was used to carry out the distribution test, which results are shown in Figure 4, with the log normal distribution having the smallest D_n value $(D_n = 0.0612)$. This method was then used to generate 50 wave data pairs with parameters: $H_{max} = 16.22$ ft, mean $= 3.45$ ft, and standard deviation $= 2.53$ ft. The wave period was determined through a linear regression of the wave period, obtaining the relationship of T to H as,

$$T = 0.5409H_s + 3.843. \tag{3}$$

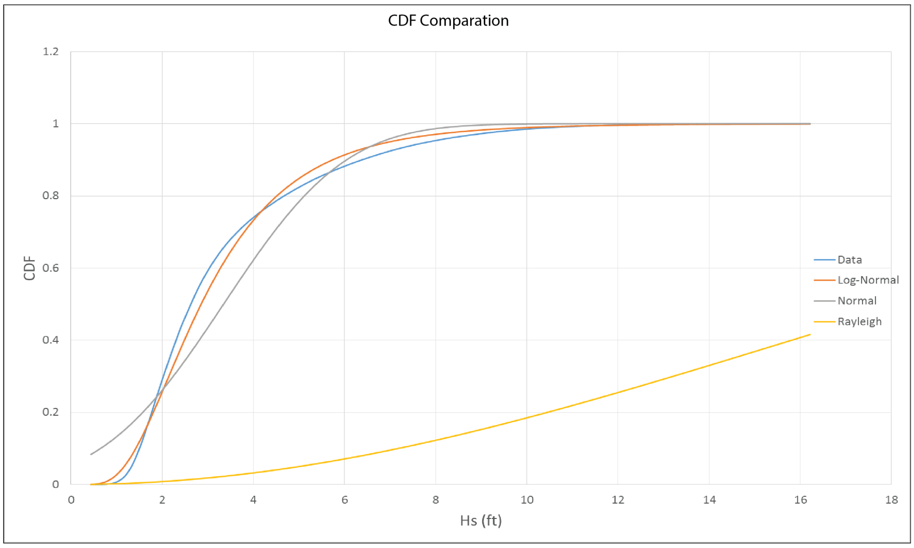

Figure 4: H_s wave K-S test results.

A period value was determined for every 50 wave heights generated. In order to generate yield stress data for the material, it is necessary to determine the statistical parameters used. ISO 19902 (2007) recommends the log normal distribution with the mean bias parameter $= 1.1266$ and standard deviation $= 0.0572$. The

location	LRFD			unfactored		
	λ_{UC}	ζ_{UC}	β	λ_{UC}	ζ_{UC}	β
main deck	-0.53	0.05	10.03	-0.98	0.05	18.20
deck leg	-1.14	0.05	21.80	-1.61	0.05	29.44
jacket	-1.34	0.08	17.62	-1.73	0.08	20.94
pile	-1.37	0.08	17.35	-1.80	0.09	20.59
		β_{average}	17.70		β_{average}	22.29

Table 14: UC statistical parameters

normal mean $F_y = 36$ Ksi is also used. The generated waveform and yield stress data are then paired as input to the Bentley SACS software. The results of the simulation yield 50 UC values for each representative member and for each pair of wave height and yield stress data generated.

A K-S test was conducted to determine the type of distribution of UC members, with the log normal distribution suitable for each member. PDF-UC factoring conditions, namely the main deck member shown in Figure 5. The probability of member failure can be determined from the PDF-UC curve by calculating the area under the PDF curve with a limit of $1 \leq UC \leq \infty$. Based on the results of the previous distribution, the calculation of the reliability index (β) was done using the following log normal equations, as follows,

$$\begin{aligned} P_f &= 1 - \Phi\left[\left(\frac{\ln(1) - \lambda_{UC}}{\zeta_{UC}}\right) - \left(\frac{\ln(0) - \lambda_{UC}}{\zeta_{UC}}\right)\right] \\ &= 1 - \Phi\left(\frac{\lambda_{UC}}{\zeta_{UC}}\right) \end{aligned} \tag{4}$$

, so we get,

$$\begin{aligned} P_f &= 1 - P_s \\ P_s &= \Phi(\beta). \end{aligned} \tag{5}$$

The value of the reliability index can be determined by,

$$\beta = \frac{\lambda_{AUC}}{\zeta_{AUC}}. \tag{6}$$

Table 13 shows the main statistical parameters of the UC obtained from the simulation results. Table 14 shows the results of calculating the reliability index value carried out on each member of the representative structure for LRFD and non-factor loading conditions. The reliability index (β) for LRFD loading conditions is 16.70 and for conditions without a factor of 22.29.

Bai (2003b) recommends P_f and values for a certain security class, as shown in Table 15. The security classes are described as low safety class, normal safety class, and high safety class. The four members that are the main focus of reliability analysis are in the category of high safety class, with the recommended minimum reliability index being 3.72. So, the reliability index value for a factored load of 16.70 without a factor of 22.3 is still very far from the recommended value range.

safety level	target (P_f)	safety (β)
Low	10^{-2}	2.32
Normal	10^{-3}	3.09
High	10^{-4}	3.72

Table 15: Environmental data.

From the results of this analysis, it was concluded that the structure of a four-legged jacket-type wellhead platform in the Java Sea, designed according to the design principles of the 1993 API RP2A-LRFD, has a very large reliability index. Further studies are needed to adjust the application of load factors to offshore platforms in Java Sea waters.

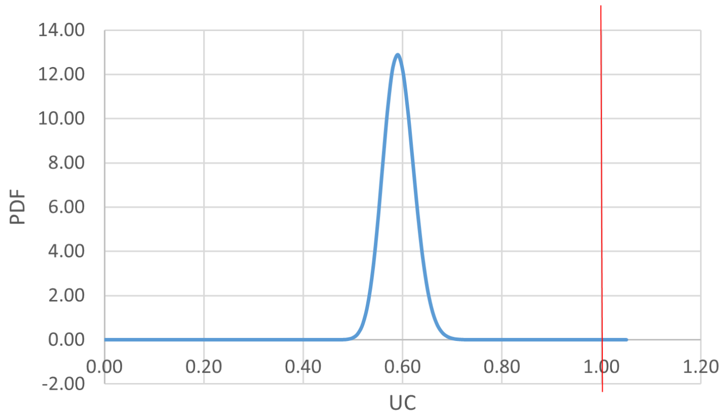

(a)

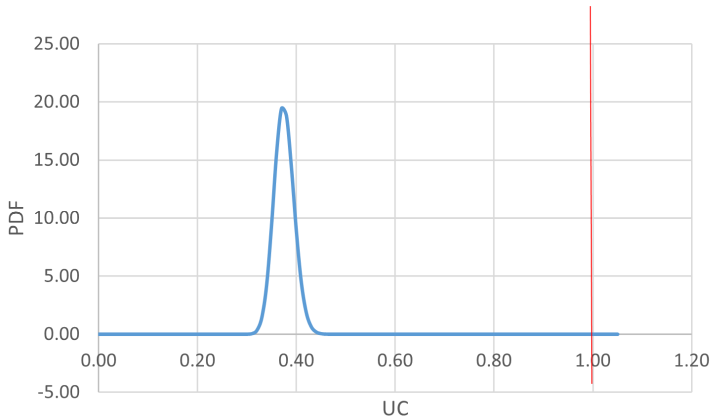

(b)

Figure 5: PDF of UC main beam: (a) LRFD and (b) unfactored.

4 Conclusion

The analysis of this study resulted in several conclusions. The structure was determined to meet the design criteria for member stress, joint punching shear, and pile capacity according to the 1993 API RP2A-LRFD design criteria. Fatigue analysis revealed one joint in the bracing to be below the desired service life of 31 years and, thus, requires optimization by increasing the cross-section. The Monte Carlo simulation method determined the reliability index (β) with 50 simulations of the four main member representatives using random variables in the form of significant waves. The mean value for the LRFD condition was 16.70, and for the unfactored condition was 22.29. It is concluded that using the 1993 API RP2A-LRFD load factor is inadequate for conditions in the Java Sea, and further studies are required to apply the appropriate load factor.

There are several suggestions to improve this study, including:

- Structure and load data for a more complete and detailed design so that the analysis results are more accurate.
- Wave data for reliability analysis should use maximum wave data to get more critical results.
- The Monte Carlo simulation is carried out more with a minimum number of 1000 simulations in order to get more accurate simulation results.
- Conduct a reliability analysis on the structure of offshore platforms in different Indonesian waters to obtain a more comprehensive conclusion regarding the study of the application of the API RP2A-LRFD environmental load factor for Indonesian waters in general.

Acknowledgements

This study was funded by ITB Research, Community Service and Innovation Program (P3MI-ITB).

References

Alpers, W. (1983). Monte Carlo simulations for studying the relationship between ocean wave and synthetic aperture radar image spectra. *Journal of Geophysical Research: Oceans*, 88(C3):1745–1759, DOI: 10.1029/JC088iC03p01745.

Bai, Y. (2003a). Chapter 18 - Fatigue Loading and Stresses. In Bai, Y., editor, *Marine Structural Design*, pages 347–362. Elsevier Science, Oxford, ISBN: 978-0-08-043921-1, DOI: 10.1016/B978-008043921-1/50018-6.

Bai, Y. (2003b). Chapter 26 - Reliability-Based Design and Code Calibration. In Bai, Y., editor, *Marine Structural Design*, pages 463–480. Elsevier Science, Oxford, ISBN: 978-0-08-043921-1, DOI: 10.1016/B978-008043921-1/50026-5.

Barthelmie, R. J., Wang, H., Doubrawa, P., and Pryor, S. C. (2016). Best practice for measuring wind speeds and turbulence offshore through in-situ and remote sensing technologies. DOI: 10.7298/X4QV3JGF.

Chen, I.-W., Wong, B.-L., Lin, Y.-H., Chau, S.-W., and Huang, H.-H. (2016). Design and Analysis of Jacket Substructures for Offshore Wind Turbines. *Energies*, 9(4), DOI: 10.3390/en9040264.

Clarindo, G., Teixeira, A. P., and Soares, C. G. (2021). Environmental wave contours by inverse FORM and Monte Carlo simulation with variance reduction techniques. *Ocean Engineering*, 228:108916, DOI: 10.1016/j.oceaneng.2021.108916.

Digre, K. A. and Zwerneman, F. (2012). Insights into using the 22nd edition of API RP 2A recommended practice for planning, designing and constructing fixed offshore platforms-working stress design. In *Offshore Technology Conference*. OnePetro, DOI: 10.4043/23558-MS.

Görmüş, T., Ayat, B., and Aydoğan, B. (2022). Statistical models for extreme waves: Comparison of distributions and Monte Carlo simulation of uncertainty. *Ocean Engineering*, 248:110820, DOI: 10.1016/j.oceaneng.2022.110820.

Guo, Y., Hou, Y., Zhang, C., and Yang, J. (2012). A background error covariance model of significant wave height employing Monte Carlo simulation. *Chinese Journal of Oceanology & Limnology*, 30(5), DOI: 10.1007/s00343-012-1278-5.

ISO 19902, N. (2007). Petroleum and natural gas industries—fixed steel offshore structures. *International Organization for Standardization*.

Karimi, H. R., KaramZadeh, N. S., and Golami, E. O. R. (2017). Effect of elevational and member damage on jacket strength: Sensitivity and reliability review of South Pars phase-20 jacket, using push-over analysis. *Ocean Engineering*, 143:209–216, DOI: 10.1016/j.oceaneng.2017.08.001.

Khatibi, E. A., Elenean, K. A., Megahed, A., and El-Hussain, I. (2014). Improved characterization of local seismicity using the Dubai Seismic Network, United Arab Emirates. *Journal of Asian Earth Sciences*, 90:34–44, DOI: 10.1016/j.jseaes.2014.04.009.

Lakhani, T. T. and Panchal, V. R. (2022). Comparative study of lifting, installation and operation analysis of subsea manifold with Mudmat structure. *International Journal of Design Engineering*, 11(2):151–159, DOI: 10.1504/IJDE.2022.130438.

Lee, G.-N., Ngo, D.-V., Lee, S.-I., and Kim, D.-H. (2023). Fatigue Life Convergence of Offshore Wind Turbine Support Structure According to Wind Measurement Period. *Energies*, 16(7):3199, DOI: 10.3390/en16073199.

Mangiavacchi, A., Rodenbusch, G., Radford, A., and Wisch, D. (2005). API offshore structure standards: RP 2A and much more. In *Offshore Technology Conference*. OnePetro, DOI: 10.4043/17697-MS.

Massey Jr., F. J. (1951). The Kolmogorov-Smirnov test for goodness of fit. *Journal of the American Statistical Association*, 46(253):68–78, DOI: 10.1080/01621459.1951.10500769.

Ozkul, S. N., Huang, W.-X., and Taxy, S. (2021). Hybrid Conductor-Supported Tripod Platform: Brownfield Design Perspective to Unlock Production Capacity. In *Offshore Technology Conference*. OnePetro, DOI: 10.4043/31157-MS.

Plodpradit, P., Dinh, V. N., and Kim, K.-D. (2019). Coupled Analysis of Offshore Wind Turbine Jacket Structures with Pile-Soil-Structure Interaction Using FAST v8 and X-SEA. *Applied Sciences*, 9(8), DOI: 10.3390/app9081633.

Qiu, L.-C. (2007). Numerical simulation of transient hydroelastic response of a floating beam induced by landing loads. *Applied ocean research*, 29(3):91–98, DOI: 10.1016/j.apor.2007.11.001.

Raheem, S. E. A., Aal, E. M. A., AbdelShafy, A. G. A., Fahmy, M. F. M., and Mansour, M. H. (2022). In-place analysis for pile structural response of fixed jacket offshore platform. *Ships and Offshore Structures*, 17(6):1224–1237, DOI: 10.1080/17445302.2021.1906039.

Sánchez, S., López-Gutiérrez, J.-S., Negro, V., and Esteban, M. D. (2019). Foundations in offshore wind farms: Evolution, characteristics and range of use. Analysis of main dimensional parameters in monopile foundations. *Journal of Marine Science and Engineering*, 7(12):441, DOI: 10.3390/jmse7120441.

Shittu, A. A., Mehmanparast, A., Hart, P., and Kolios, A. (2021). Comparative study between SN and fracture mechanics approach on reliability assessment of offshore wind turbine jacket foundations. *Reliability Engineering & System Safety*, 215:107838, DOI: 10.1016/j.ress.2021.107838.

Tran, T.-T., Kim, E., and Lee, D. (2022). Development of a 3-legged jacket substructure for installation in the southwest offshore wind farm in South Korea. *Ocean Engineering*, 246:110643, DOI: 10.1016/j.oceaneng.2022.110643.

Turner, R. C., Ellinas, C. P., and Thomas, G. A. N. (1994). Worldwide Calibration of API RP2A-LRFD. *Journal of Waterway, Port, Coastal, and Ocean Engineering*, 120(5):423–433, DOI: 10.1061/(ASCE)0733-950X(1994)120:5(423).

Uieda, L., Tian, D., Leong, W. J., Schlitzer, W., Grund, M., Jones, M., Fröhlich, Y., Toney, L., Yao, J., Magen, Y., Tong, J.-H., Materna, K., Belem, A., Newton, T., Anant, A., Ziebarth, M., Quinn, J., and Wessel, P. (2023). PyGMT: A Python interface for the Generic Mapping Tools. DOI: 10.5281/zenodo.7772533.

Wessel, P., Luis, J. F., Uieda, L., Scharroo, R., Wobbe, F., Smith, W. H. F., and Tian, D. (2019). The Generic Mapping Tools Version 6. *Geochemistry, Geophysics, Geosystems*, 20(11):5556–5564, DOI: 10.1029/2019GC008515.